Introduction

The time-reversal method (Fink 1992 and 1993) allows a very efficient approach to focus pulsed waves through inhomogeneous media. In time-reversal acoustics, a signal is recorded by array of receivers, time-reversed and then re-transmitted into the medium. The re-transmitted signals propagate back through the same medium along both the direct waves and multiple scattering paths and refocus on the source. Time reversal method is similar to the seismic migration concept described by Whitmore (1983) and McMechan (1983).

Two kinds of time-reversal are defined: the time reversal cavity (TRC) and the time reversal mirror (TRM). In the TRC the array of receivers completely surrounds the source and thus the time-reversed signals propagate backwards through the medium and retrace their primary and multiple scattering paths that they propagated in the forward direction. In the TRM, the array of receivers covers a limited area and just a smaller part of the field is captured.

Several publications described lab and field TRM experiments such as Kuperman et al. (1998) and Song et al. (1998) using sonic waves in the ocean, de Rosny and Fink (2002) using acoustic waves in a laboratory experiment, Leorosey et al. (2007) using EM waves, and Hanafy el al. (2009) using seismic waves. Hanafy et al. (2009) used TRM to find the location and excitation time of unknown seismic sources in the subsurface. One of the geophysical applications of this method was to locate trapped miners in collapsed mines. Results showed that TRM can be used to accurately locate trapped miners even with data having a very poor signal to noise ratio. In this work, we discuss a new geophysical application of seismic TRM; track moving objects within an area of interest. Before tracking moving objects, calibration TRM records are required. These records will be used to track moving objects, and should be recorded beforehand with a high signal-to-noise ratio (SNR).

Theory

Hanafy et al. (2009) showed that the time reversal mirrors is equivalent to standard poststack migration except that trial time shifts are introduced into seismic records to compensate for the unknown source point and excitation time. The migration images (obtained by poststack migration of passive seismic data from buried point source) are compared for different time shifts and the localized maxima of migration amplitudes pinpoints the unknown source locations. The migration image $m(\boldsymbol{x}, t)$ is given by

$$m(\boldsymbol{x}, t) = \sum d(\boldsymbol{g}, \tau | \boldsymbol{s}, t_{source}) * G(\boldsymbol{x}, -t | \boldsymbol{g}, 0) \qquad (1)$$

where $d(\boldsymbol{g}, \tau | \boldsymbol{s}, t_{source})$ represents the passive data recorded at time $\tau = \tau_{xg} + t$ and at receiver location $\boldsymbol{g}$ for a source at $\boldsymbol{s}$ with unknown excitation time t_{source}; and τ_{xg} is the traveltime from $\boldsymbol{x}$ to $\boldsymbol{g}$. Here, the variable *t* is the trial time shift to compensate for a non-zero excitation time, and $\boldsymbol{x}$ is the trial image position. Choosing the trial time $t \rightarrow t_{source}$ and trial source location $\boldsymbol{x} \rightarrow \boldsymbol{s}$ yields the maximum migration image at the actual source location $\boldsymbol{s}$ (Hanafy et al., 2009).

In this paper, a group of receivers is permanently buried in the area of interest. A number of stations $\boldsymbol{x}$ (in equation 1) are then selected and from each station one reference Green's function ($G(\boldsymbol{x}, -t | \boldsymbol{g}, 0)$ in equation 1) with a high signal-to-noise ratio is recorded. In practice, a metal plate is located at $\boldsymbol{s}$ and recorded traces are stacked together from repeated hammer blows to the plate. Later, the same group of receivers will continuously record any passive seismic activity and send it to the processing station to monitor any abnormal activities in the area of interest. Here, both the excitation times and the source locations are unknown. In this case, equation 1 is used to find the excitation times and source locations, where $G(\boldsymbol{x}, t | \boldsymbol{g}, 0)$ represents the previously recorded Green's functions and $d(\boldsymbol{g}, \tau | \boldsymbol{s}, t_{source})$ represents the passive seismic data.

Correlation results from equation 1 are contoured and rendered as 2D maps, where each map corresponds to a certain time snapshot. Local maximum that exceeds a pre-selected threshold value

pinpoints the location of the moving object, while the snapshot time's value represents when the moving object was at that location. Repeating this process for different time intervals gives the location of the moving objects at different times. The velocity of the moving object can be approximately found based on this information.

The inline and crossline offsets between the receivers/shots do not need to be uniform; however, it is important to have a sufficiently dense coverage of both receivers and calibration shots to accurately locate the moving object. The required density can be estimated by computerized experiments, but a good criterion might be a sampling interval of $\lambda/2$. Processing time is very fast, thus allowing almost real time monitoring of the area of interest.

Field Data Test

The application of tracking moving objects is tested with field data. The seismic data are collected at Tucson, AZ., where five parallel receiver lines are used with 5 m receiver intervals and 15 m line interval (Figure 1). Each line contains 24 receiver points, and one reference Green's function is recorded at each receiver point (Figure 2a) by repeatedly hammering a metal plate on the ground and stacking the resulting traces together. These Green's functions are used in equation 1 to track moving objects in the area of study. A man moved in the study area following four different routes (Figure 1). He was walking in the first two routes (Figures 1a and 1b) and running in the other two routes (Figure 1c and 1d). We continuously recorded the seismic signals (Figure 2b) during his movement and used the previously recorded Green's functions to track the moving person inside the study area.

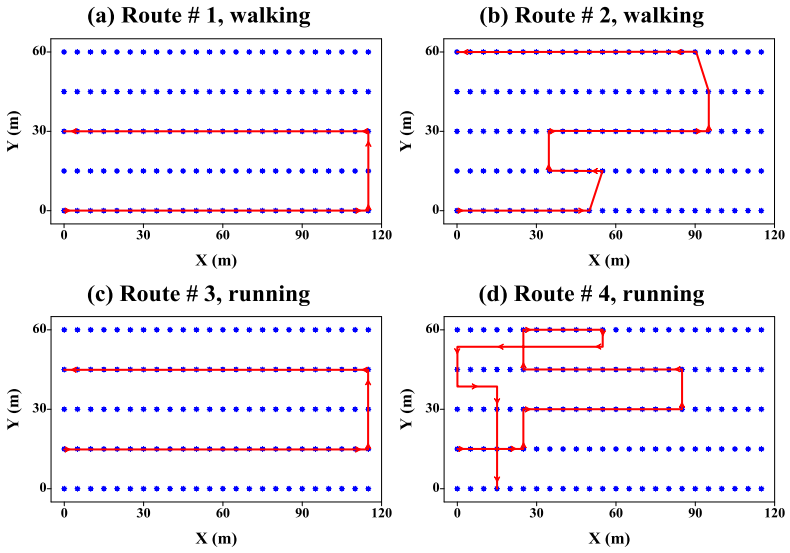

Figure 1 *A base map shows data collection in Tucson, AZ. USA. Blue points represent receiver locations; one Green's function is collected at each receiver location. Red line represents route taken by the moving person, in (a) and (b) he was walking, while in (c) and (d) he was running.*

Figure 3 shows selected snapshots from the correlation results of routes 2 as an example of the results. The snapshots are selected so that they show the walker when he is next to one of the geophones. Figure 3 shows that we can accurately track the location of the moving object in the area.

To find the velocity of the walker we selected part of the path where the walker was moving in a straight line. The velocity, *v*, of the walker is determined by $v = r/t$, where *r* is the distance between two points along the walker track and *t* is the time required to move between these two points. We calculated two velocity values for the given field example (route 2) and two velocity values for route 3 (not shown here) as an example when the person was running in the site, the results are:

- *Route 2, part 1*. The distance between stations 2 and 11, Figures 3a and 3b, respectively, is 45 m and the time the walker takes to move between these two stations is 17.7 s, which gives a velocity of approximately 2.5 m/s.

- *Route 2, part 2*, the distance between stations 108 and 98, Figures 3g and 3h, respectively, is 50 m and the time the walker takes to move between these two stations is 17.5 s, which gives a velocity of approximately 2.9 m/s.
- *Route 3, part 1*, the distance between stations 25 and 46 is 105 m and the time the runner takes to move between these two stations is 21.1 s, which gives a velocity of approximately 5 m/s.
- *Route 3, part 2*, the distance between stations 87 and 74 is 65 m and the time the runner takes to move between these two stations is 11.9 s, which gives a velocity of approximately 5.5 m/s.

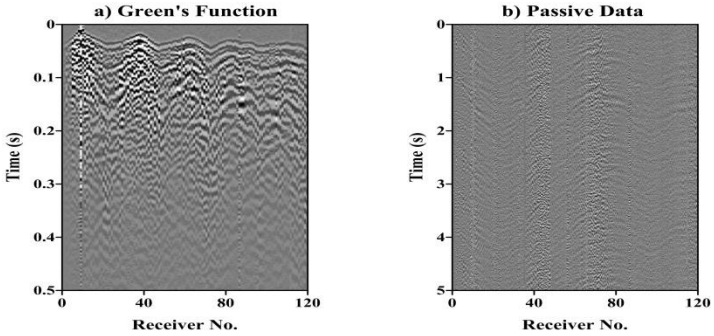

Figure 2 *a) Green's function for a shot at station 10 and b) data recorded for a human walking along route 2.*

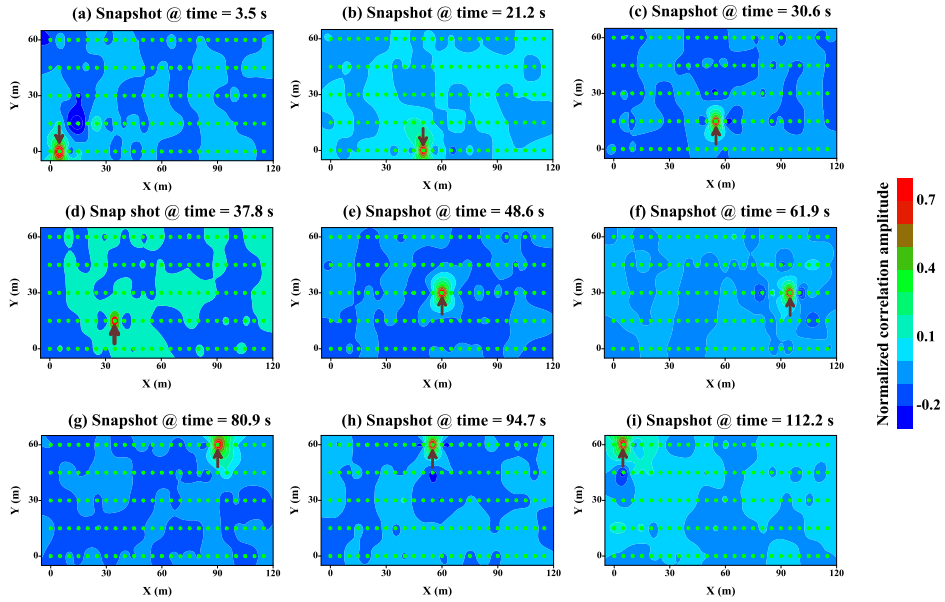

Figure 3 *Snapshots at different times show the correlation results for a walking human along route 2. Location of the walking human is characterized by high correlation values (red colour). Brown arrow refers to the actual location of the walking human.*

Accuracy Test

To find how close the moving object should be to a receiver/shot point to accurately track it, we selected the snapshot at time 48.6 s from route 2. Here, the moving object was next to station 61 (Figure 4a). Figures 4b-4f show five snapshots with 0.45 s time interval between each two successive snapshots. In Figures 4b to 4f, all amplitudes are normalized with respect to the values in Figure 4a. In Figure 4a, the maximum amplitude is exactly at station 61. In Figure 4b, which is 0.45 s later and the walking person is around 1 m away from station 61, the maximum amplitude value is still at station 61, but its value is less than that at Figure 4a. Moving away from station 61 will gradually decrease the correlation amplitude value, until we are close enough to station 62, where a new peak is formed.

This test shows that, the maximum correlation value occurs when the moving object is exactly at receiver/shot location, moving away from that location decreases the correlation value, and if the distance between receiver/shot points is too large, we may not be able to accurately locate the moving object. This problem can be eliminated by using a finer sampling of source points when creating the calibration Green's functions. The optimum offset between receiver/shot point depends on the site

condition, sampling interval of the calibration Green's functions, background noise, and signal-noise ratio of the reference Green's function. The frequency response of the receivers could be a factor in accuracy, but we did not test this in the current work.

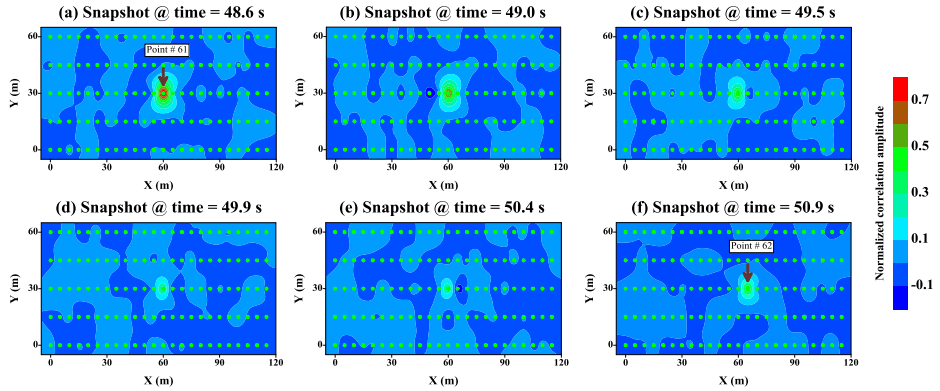

Figure 4 *Snapshots show the correlation result when the moving object is: a) at station 61, and b) to f) the following five shots with 0.45 s time intervals between each two.*

Conclusions

In this paper we presented how to remotely track moving objects by TRM. A group of receivers are buried in the area of interest and continuously record the passive seismic data from any moving object in that area, which is very similar to tracking moving objects with radar, however, here we use seismic signals and not EM waves. The passive data are correlated with the previously recorded calibration Green's function and the high amplitude value refers to the location of the moving object. Tracking moving objects can be done in almost real time and the approximate velocity of that object can be easily calculated.

One field tests is carried out in Tucson, AZ to test the proposed TRM application. Results show that the location and velocity of moving objects can be accurately found. This assumes that we have dense enough shot locations with high signal-to-noise ratio Green's functions.

Acknowledgements

The author would like to thank Mr. Paul Gettings and Mr. Ernesto Curiel for the help they provided during field data acquisition.

References

de Rosny, J. and Fink, M. [2002] Overcoming the diffraction limit in wave physics using a time-reversal mirror and a novel acoustic sink. Physical Review Letters, **89**, 124301-1 - 124301-4.

Fink, M. [1992] Time reversal of ultrasonic fields: basic principles. IEEE Trans. Ultrason. Ferroelectr. Freq. Control **39**, 555-566

Fink, M. [1993] Time-reversal mirrors. J. Phys. D: Appl. Phys, **26**, 1333-1360.

Hanafy, Sh.M., Cao, W. and Schuster, G.T. [2009] Using super-stacking and super-resolution properties of time-reversal mirrors to locate trapped miners. The Leading Edge, **28**, 302-307.

Kuperman, W.A., Hodgkiss, W.S., Song, H.C., Akal, T., Ferla, C. and Jackson, D.R. [1998] Phase conjugation in the ocean: experimental demonstration of an acoustic time-reversal-mirror. J. Acoust. Soc. Am., **103**, 25 - 40.

Lerosey, G., de Rosny, J., Tourin, A. and Fink, M. [2007] Focusing beyond the diffraction limit with far-field time reversal. Scince, **315**, 1120-1122.

McMechan, G. A. [1983] Migration by extrapolation of time dependant boundary values. Geophysical Prospecting, **31**, 413 - 420.

Song, H. C., Kuperman, W.A. and Hodgkiss, W.S. [1998] A time-reversal mirror with variable range focusing. J. Acoust. Soc. Am, **103**, 3234 - 3240.

Whitmore, N. D. [1983] Iterative depth migration by backward time propagation. Expanded Abstracts of SEG, 382 - 385.